International Journal of Minerals, Metallurgy and Materials
Accepted manuscript, https://doi.org/10.1007/s12613-019-1929-z

Characterization of microstructural changes and reactivity of mechanically activated ilmenite

H. Ebadi[a], P. Pourghahramani[b,*], B.N. Akhgar[c]

[a] Mining Engineering Department, Sahand University of Technology, P.O. Box 51335/1996, Tabriz, Iran

[b,*] Mining Engineering Department, Engineering Faculty, Sahand University of Technology, P.O. Box 51335l1996, Tabriz, Iran

[c] Mining Engineering Department, Engineering Faculty, Urmia University, P.O. Box 57561/51818 Urmia, Iran

Abstract

Structural changes and reactivity of mechanically activated ilmenite concentrate during milling by a planetary mill were monitored and determined as a function of milling time. The maximum specific BET surface area of 10.76 m^2/g was obtained after 150 min of milling. The results indicated that agglomeration of particles occurred after 45 min of milling. The maximum X-ray amorphization degree ca. 95% was calculated after 150 min of milling. The estimation of stored energy revealed that the x-ray amorphization degree has a dominant contribution on the excess enthalpy of activated materials. The surface-weighted crystallite size in ground ilmenite reaches to 4.45 nm which corresponds to the volume-weighted crystallite size of 8 nm and 11.18 nm obtained by Williamson-Hall and Rietveld methods, respectively. After 150 min of mechanical activation, the root mean square strain, $< \varepsilon^2_{L=10nm} >^{1/2}$ increased to 0.78%, which corresponds to strain of 1.43% and 1.04% obtained from Williamson-Hall and Rietveld methods, respectively. Reduction of crystallite size leads to contraction of the ilmenite unit cell after 150 min.

The reaction rate constant of ilmenite dissolution increased by over 58 times after 150 min of milling. Activation energy of dissolution reaction decreased from 57.45 kJ/mol to 41.09 kJ/mol after 150 min of milling.

Keywords: Ilmenite; Mechanical activation; Structural changes; XRD line profile analysis; Reactivity

* Corresponding author at : Mining Engineering Department, Engineering Faculty, Sahand University of Technology, Tabriz, Iran. Tel. : +984133459289
E-mail address: Pourghahramani@sut.ac.ir (P. Pourghahramani).

1. Introduction

Mechanical activation refers to a process wherein, large amounts of energy are mechanically transferred to the materials during high-energy milling whereas chemical composition of the involved materials remains unchanged[1].

As a result, after mechanical activation these materials possess high entropy, high free energy and high tendency to contribute in a reaction [2-4]. It is well known that mechanical activation is useful to increase the reactivity of minerals during leaching process, sintering, smelting and production of Nano-minerals with special properties [2].

Ilmenite as a fairly refractory mineral with chemical composition of $FeTiO_3$ is the primary source of titanium metal and other titanium-bearing components such as precious white pigment (TiO_2). This oxide mineral, bearing high resistance against decomposition, can be considered as a strategic mineral in manufacturing of titanium metal which has advanced high-tech applications. There are several approaches for extraction of TiO_2 from ilmenite such as sulfate and chloride processes, presently producing around 40% and 60% of the world's TiO_2 pigments, respectively [5, 6]. Both processes are expensive and complicated with serious environmental problems. Therefore, in last decades, many researches attempted to modify the mentioned processes by using new treatment techniques such as mechanical activation method. Microstructural changes and phase transformation of mechanically activated ilmenite has been studied for different cases. The obtained results of microstructural changes and phase transformation during the mechanical activation are different. Welham and Llewellyn [7] have reported that as ilmenite was mechanically activated in conventional ball mill for more than 100 h, crystallite size decreased and lattice strain increased without any detectable phase transformation. On the other hand, Chen [8] reported gradual conversion of ilmenite to pseudo-rutile ($Fe_2Ti_3O_9$) during mechanical activation under air atmosphere after 200 hours of milling by a planetary ball mill. Previous investigations have been generally focused on study of the effects of mechanical activation in different milling conditions, on dissolution rate of ilmenite during leaching by the sulfuric or hydrochloric acids [5-12]. The results revealed that intensive milling process increases the dissolution rate of ilmenite. A detailed literature survey indicates that the milling of ilmenite concentrate produces a nano-crystalline structure with different levels of micro-strain. The difference in results could be attributed to different milling conditions, various ilmenite sources and using unsophisticated microstructural characterization approaches which leads to large errors in the calculation steps of microstructural characteristics. Unfortunately, to best of our knowledge, the microstructural changes of ilmenite during mechanical activation are not studied exclusively using professional methods of microstructural analysis. In addition, in the conducted studies, calculation of some important parameters such as the X-ray amorphization degree have been ignored whereas the X-ray amorphization degree is considered as the most important microstructural parameter regarding atomic bonds strength. It is well known that more than 90% of stored energy in the structure of mechanically activated materials relates to the

amorphization [13]. As a result, the underlying factors behind the changes in the reactivity of the mechanically activated ilmenite could not be fairly comprehended, because changes in the reactivity of the mechanically activated materials during steps of a process depends largely to the available structural characteristics at each step of the process [14, 15], an exact structural refinement approach and data collection before making any interpretation is of prime importance.

The main objective of this paper is to investigate the effect of mechanical activation process on the microstructural changes and reactivity of Iranian ilmenite concentrate during milling by high energy planetary ball mill using X-ray diffraction profile analysis. Williamson-Hall (W-H), Warren-Averbach (W-A) and Rietveld methods were used for precise determination of crystallite size and lattice strain. In the following, dislocation density, change in lattice volume and stored energy were calculated for mechanically activated ilmenite. In addition, an insight into the reactivity of mechanically activated ilmenite concentrate in the initial process of TiO_2 pigment production is elucidated.

2. Experimental

2.1. Material

Ilmenite concentrate was kindly supplied from flotation pilot plant of Ghara-aghaj polymetallic ore. Ghara-aghaj titanium deposit has been located in the 36 Km at the North-West of Euromieh, Iran. Mineralogical study of concentrate by using an optical microscope indicates presence of Magnesium-Hornblende as main gangue mineral remaining in the concentrate. Analysis of obtained XRD patterns (Fig. 1) revealed mainly ilmenite reflection peaks, corresponding to JCPDS NO. 01-075-1210. The reflection peak at $2\Theta=28.7^{\circ}$ is related to Magnesium-hornblende, which is corresponding to JCPDS NO. 00-045-1371. The chemical analysis of ilmenite concentrate indicates that the concentrate comprises of 45.50% TiO_2 (Table **1)**.

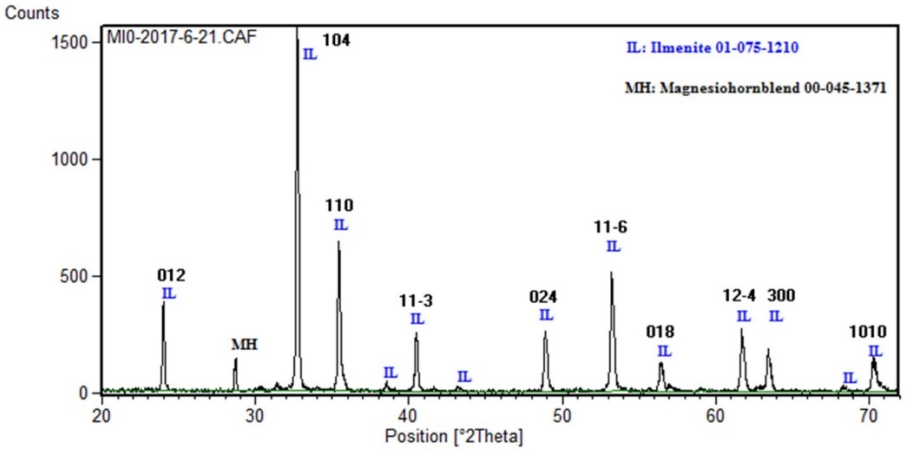

Fig. 1. XRD pattern of ilmenite concentrate

Table 1

Chemical composition of ilmenite concentrate

Oxide	TiO_2	Fe_2O_3	SiO_2	Al_2O_3	CaO	MgO	MnO	P_2O_5	Cr_2O_3	Na_2O	LOI	Total
(Wt %)	45.22	50.21	3.43	0.35	0.37	2.32	0.88	0.12	0.02	0.2	-3.12	100

2.2. Characterization

The untreated and mechanically activated samples were characterized using XRD, laser particle size analysis, BET surface area measurements and SEM analysis. The XRD patterns were collected by an X-ray powder diffractometer (Bruker Axs D8, Germany) using Cu Kα radiation (λ = 1.5406 Å) at 40 kV and 40 mA. The 2Θ range of 20–72°, step size of 0.02° and counting time of 3 second were used for all records. The X-ray diffraction patterns were indexed using JCPDS (Joint Committee on Powder Diffraction Standards) files. Winfit software [16] was used to line profile analysis of XRD patterns to extract XRD line parameters. A laser diffraction instrument (Mastersizer 2000, Malvern, UK) was employed for particle size analysis of samples in order to measure of granulometric surface area and mean particle size. Belsorp mini II (Microtrac BEL Corp, Japan) was employed to measure of specific surface area of the activated and non-activated samples using the BET method. SEM images were obtained by a scanning electron microscopy (VEAGA-SEM TS5136MM, Czech Republic) in the backscatter electron imaging mode. Chemical analysis of Ti value in the leaching solution was carried out using Ultraviolet-visible spectroscopy (SPECORD 200, Germany).

2.3. Mechanical activation

Ilmenite samples were activated in a planetary ball mill (Pulverisette 6, FRITSCH, Germany) by applying a rotation speed of 450 rpm. Ball to powder weight ratio of 15:1 and twelve stainless steel balls with diameter of 19 mm were used in the milling process. Mechanical activation of samples was carried out for 20, 45, 90 and 150 min. To reduce the sticking of powder to the milling media and cup, milling was stopped at the given milling intervals and powders were softened. The obtained powder samples were sealed and kept in a freezer.

2.4. Leaching experiments

A series of leaching experiments were carried out using sulfuric acid of 50% (w/w) concentration to assessment mechanical activation effect on reactivity of ilmenite. For leaching experiments, a 250 ml three neck flat bottom flask equipped with a reflux condenser and a thermometer was used. For each test, firstly 250 ml of sulfuric acid were poured in the flask and levelled to the desired temperature by hot plate. Then, 2.50 g of sample was introduced to the acid solution and stirred by a magnet stirrer.

2.5. Profile fitting

Profile fitting is the first step in microstructural characterization of X-ray diffraction pattern to extract XRD line parameters. In profile fitting, firstly the $K\alpha_2$ component of peak profile was removed, $K\alpha_1$ intensity is double of the $K\alpha_2$ intensity, and in the next the profile backgrounds was subtracted and the overlapped peaks were resolved. The peaks of (012), (104), (110), (11-3), (024), (11-6), (12-4) and (300) related to ilmenite diffraction was selected for determination of microstructural data using line profile analysis. XRD line profiles of activated, non-activated and standard LaB_6 samples were fitted by combination of Cauchy and Gaussian functions. A typical profile fitting to the XRD pattern is shown in **Fig. 2**.

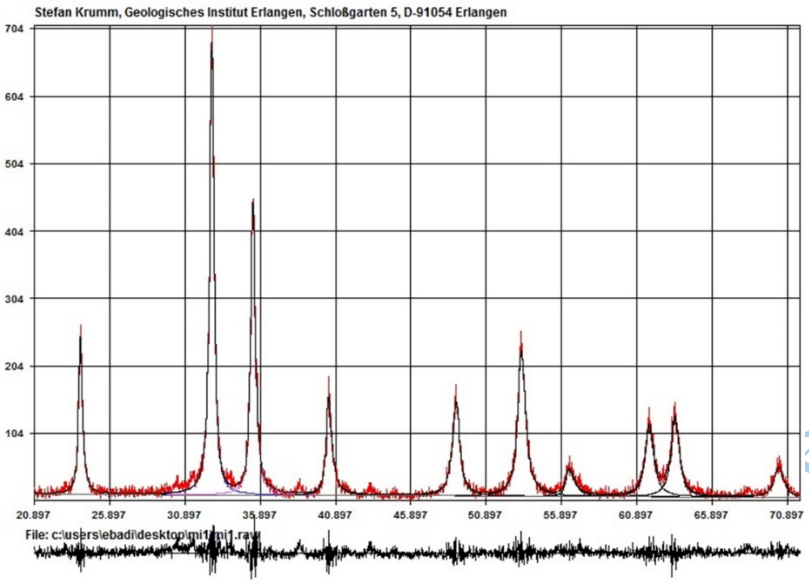

Fig. 2. A typical profile fitting of XRD diffraction pattern for 20 min mechanically activated ilmenite. The observed, measured patterns and their differences are pictured

2.6. Microstructural characterization

Any imperfection in the crystal structure cause changes in the XRD pattern background, peaks position, diffraction peaks intensity and broadness of diffraction peaks. Broadness of a peak is related to lattice strain and crystallite size and these parameters can be calculated by W-H equation as bellow:

$$\beta_{hkl}\cos\theta_{hkl} = \frac{K\lambda}{D_v} + 4\varepsilon\sin\theta_{hkl} \qquad 1$$

Where β_{hkl} is physical broadening of the peak, θ is the Bragg angle of the (h k l) peak, λ is the wavelength of used X-rays, D_v is the crystallite size, ε is the lattice strain and K is a constant. More detailed information about k has been given by Langford and Wilson [17]. The intercept and slop of the plot of $\beta_{hkl}\cos\Theta_{hkl}$ as a function of $4\varepsilon\sin\Theta_{hkl}$ (W-H plot) are used for calculation of the lattice strain and domain size, respectively.

The W-A analysis is based on the measurement of the structural broadening of two (or more) reflection peaks from the same crystallographic planes. W-A method separate the effect of crystallite size and root mean square strain (RMSS) by fitting of the Fourier series to the peak profiles. Detailed explanation of the approach are given in our previous study [18]. More detailed information about W-A method was given by Warren [19] and summarized by Bourniquel et al. [20].

Rietveld analysis is another practical method for microstructural characterization of materials. Principles of Rietveld analysis have been presented by H.M. Rietveld [21]. This method uses crystallographic data for simulating of X-ray diffraction pattern via full profile fitting of a measured XRD pattern. Fitting goodness is measured by Eq. (2) [22].

$$R = \sum_i W_i \left[y_i\,(obs) - y_i\,(calc) \right]^2 \qquad (2)$$

where $y_i\,(obs)$ is the observation intensity, $y_i\,(calc)$ is the calculated intensity and W_i is a coefficient that equals to $1/y_i(obs)$. The R values for the analysis in the present work were obtained less than 10 and close to 1 which signifies a good fit.

X'Pert High Score Plus software[23] was used for Rietveld analysis in this work. A typical profile fitting by Rietveld method on a XRD pattern of mechanically activated ilmenite is shown in **Fig. 3**.

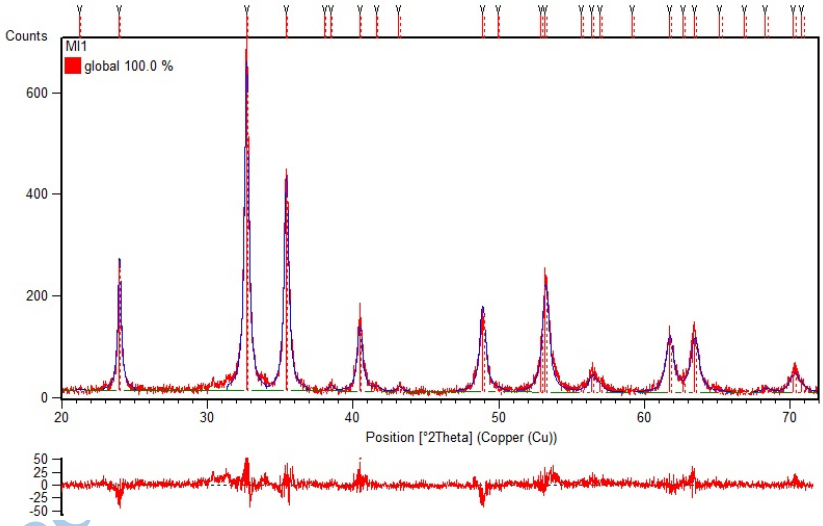

Fig. 3. Rietveld analysis of activated ilmenite. Measured profile (red line) and calculate profile (blue line) are shown in figure.

3. Result and discussion

3.1. Size distribution and morphology of particles

Granulometric and BET specific surface area are the main characteristic parameters which are subjected to significant change during mechanical activation. The obtained results are shown in **Fig. 4** emphasize on variations. BET surface area increases with milling time, up to 16 times and in the final stage reaches to maximum value of 10.76 m^2/g. Granulometric surface area increases rapidly from 0.55 m^2/g for unmilled ilmenite concentrate to 5.85

m^2/g after 20 min milling. However, by extending milling, its value falls to 4.26 m^2/g after 90 min milling and increases again to 6.53 m^2/g in 150 min milled sample. The simultaneous decrease in granulometric surface area and increase in BET surface area implies the agglomeration of particles. These agglomerated particles are porous and accessible for nitrogen gas in the BET analysis so the BET specific surface area increases as the granulometric surface area decreases. The particle size distributions are compared in **Fig. 5**. It is clear that the activated sample for 20 min yields the finest product. Prolonged milling leads to the re-welding and agglomeration of the particles and the further size reduction is impossible. Agglomeration phenomena causes the particles size distributions from prolonged milling move toward larger sizes. It could be expected that the agglomeration continues with the extended milling. The similar results are reported in previous investigations for hematite, activated in a vibratory mill [18], for pyrite, activated in a planetary mill [24], and for olivine, activated in Spex mill [25] suggesting that the agglomeration is a Probable phenomenon in dry milling process.

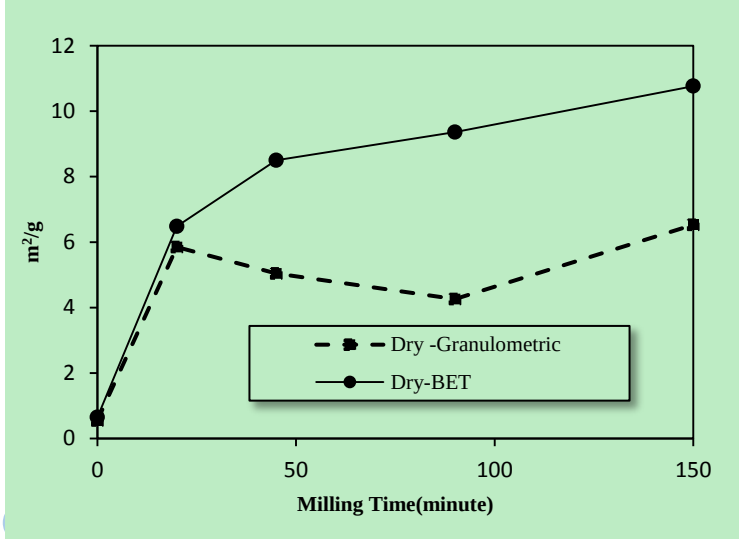

Fig. 4. BET and Granulometric surface area variation with milling time.

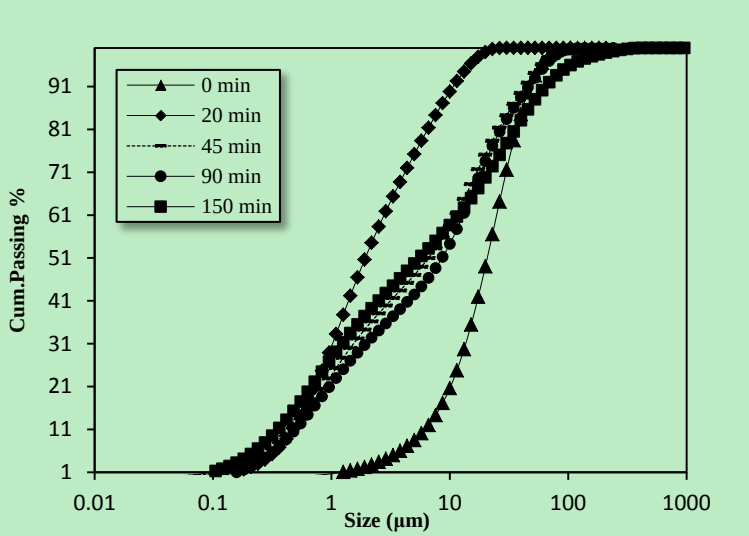

Fig. 5. Particle size distributions of un-milled and mechanically activated ilmenites

SEM images of unmilled and milled ilmenite concentrates are shown in **Fig. 6**. Unmilled ilmenite particles are completely angular with different sizes and fracture surfaces. It can be seen that with the formation of strong clusters, the agglomeration occurs by prolonged milling. It is clear that the agglomerated particles are dens in the initial stage of milling (45 min a & b) and by extending the milling time, the particles were ground again and agglomerated flaky particles with low density has been produced. The results are in agreement with the surface area measurements and particle size distributions.

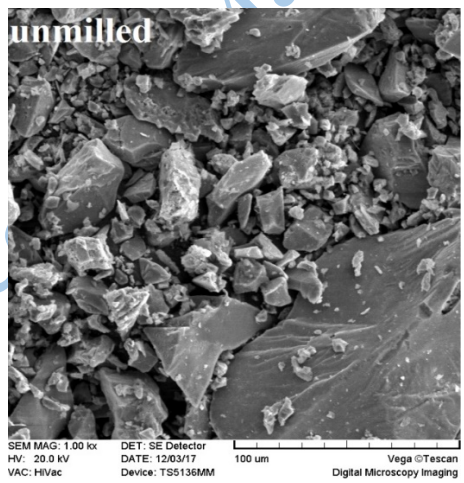

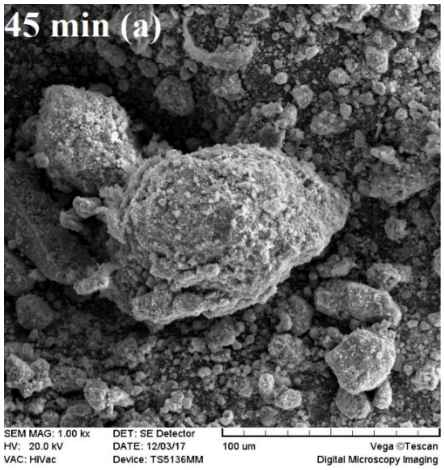

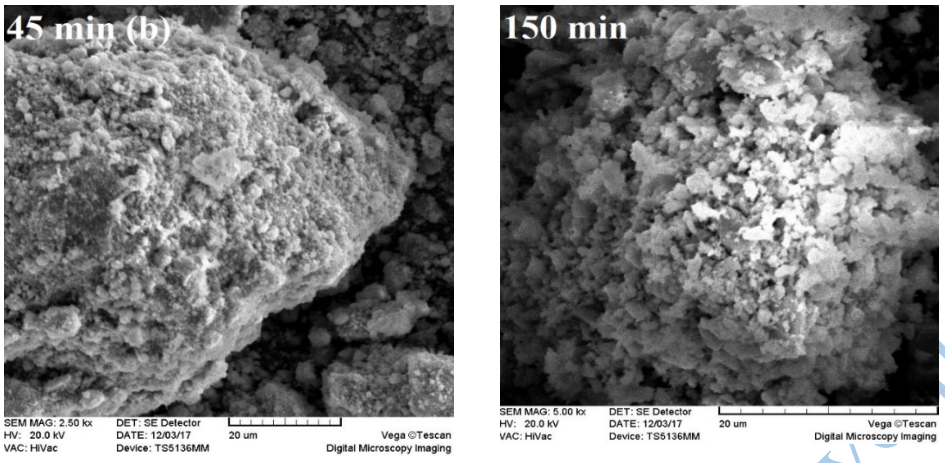

Fig. 6. SEM image of unmilled and milled ilmenite for different time and magnification.

3.2. X-ray diffraction

XRD profiles of activated and non-activated ilmenite samples are represented in **Fig. 7**. All the patterns indicate hexagonal structure of ilmenite phase, matching the standard XRD pattern of hexagonal structure $FeTiO_3$. The peak related to Magnesium-Hornblende mineral (2Θ=28.7°) disappeared after 20 min of milling. XRD analysis did not revealed any new crystalline phase formation. Based on the report of Sasikumar et al. [10], the traces of pseudo-rutile cannot be detected in XRD patterns duo to amorphization. There is no evidence for the formation of pseudo-rutile in the obtained XRD pattern. On the other hand, from macroscopic visualization, it was found that the color of milled samples for 90 and 150 min are different from the unmilled ilmenite. The changes in powder color is probably due to the surface oxidation of ilmenite, as cited before, ilmenite milling in air leads to oxidation [8]. Li et al. [9] provides more evidence by TG analysis, as a portion of the Fe atoms of the activated ilmenite was oxidized during the mechanical activation.

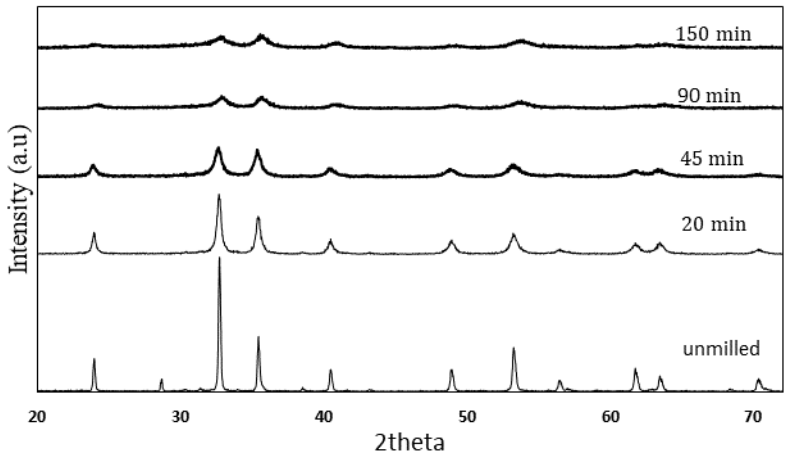

Fig. 7. XRD patterns of the unmilled and mechanically activated ilmenite for different milling times.

High-energy ball milling of ilmenite concentrate results in peaks broadening, changes in peaks position and decreases in peaks intensity (Fig. 8). Disordering of material structure due to of the formation of the amorphous material is revealed by decrease in the integral intensity of diffraction lines. The broadening of the diffraction peaks is due to of the plastic deformation and breakdown of particles as it is obvious with increasing mechanical activation time. In the case of prolonged milling time, these changes are more significant. Fig. 8 shows that the diffraction peaks of ilmenite almost disappear after 150 min of mechanical activation. Comparing with results of other researches [5-7, 9-11], it appears that the changes in the microstructural parameters of mechanically activated ilmenite could be more intensive in this study due to the intensive treatment conditions.

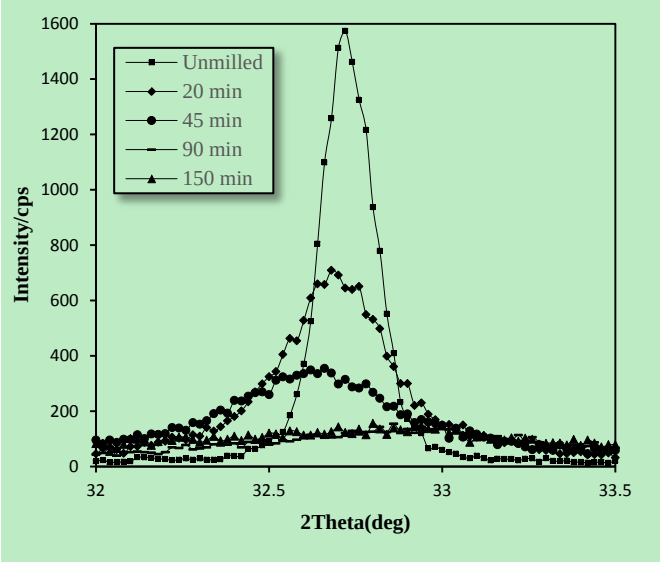

Fig. 8. Variation of peak broadening, 2theta and intensity of main peak (104) of unmilled and mechanically activated ilmenite.

3.3. Microstructure characterization

Microstructure characterization of ilmenite concentrate and mechanically activated samples were carried out by W-H, W-A and Rietveld methods. Williamson-Hall plots were depicted using Eq. (3) and the results are illustrated in Fig. 9. The volume weighted crystallite size (D_v) and lattice strain were calculated using Williamson-Hall plots. With increasing milling time, the slope and intercept of plots increases continuously but at milling times more than 90 min, the slop of plots are approximately remained unchanged. From the results, it can be concluded that the crystallite size decreases continuously and the lattice strain reaches to maximum value by 90 min and then remains almost constant. Rietveld and W-H results are in line with each other, implying the the validity of the obtained results. W-H method estimates larger lattice strain in comparison to Rietveld method. This trend has also been reported by Jiajie Li and Michael Hitch [25] for mechanically-activated olivine.

In addition, the microstructural characteristics were determined using W-A based on Fourier transformation of the XRD lines and the obtained results are compared in Table 2. It can be observed that the surface-weighted crystallite size in ground ilmenite is 4.45 nm after 150 min in the planetary mill, corresponding to the volume-weighted crystallite size of 8 nm. After 150 min mechanical activation, the root mean square strain, $< \varepsilon^2_{L=10nm} >^{1/2}$ increases to 0.78%, corresponding to strain of 1.43% obtained from Williamson-Hall approach.

The results of W-H and W-A methods must be in limited range based on the line profile shape. If the broadened strain contains a Cauchy component, there will be no a clear correlation between *RMSS* and ε. Balzar [26] presented a rough estimation as Eq. (3) when the Cauchy and Gauss extremes of the strain broadened Voigt profile exist:

$$0.5 \leq \frac{\varepsilon}{< \varepsilon_l^2 >^{\frac{1}{2}}} \leq \qquad (3)$$

On the other hand the relationship between D_v and D_s for a Voigt size-broadened profile are given by:

$$1.31 \leq \frac{D_v}{D_S} \leq \qquad (4)$$

For other methods;

$$\frac{D_v}{D_S} \leq r \qquad (5)$$

In the present work the value of Eq. (3) for calculated strain results using W-H and W-A methods varies in range of 1.26-1.84. Therefore it could be concluded that W-H and W-A method results are in good agreement with each other. In addition, D_v/D_s for crystallite sizes is in the range of 1.44-2.67.

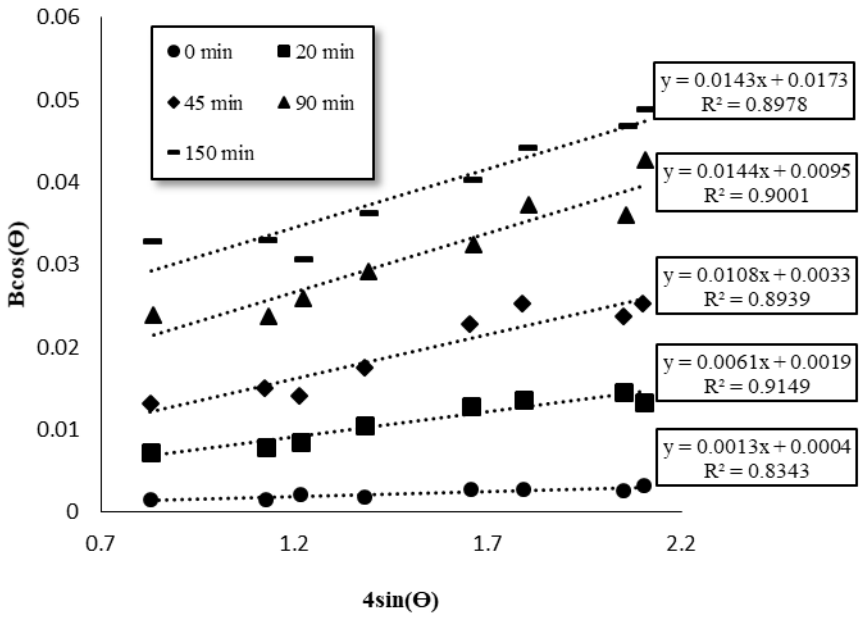

Fig. 9. Williamson–Hall plots for ilmenite concentrate samples milled with different time.

Table 2

Microstrain and crystallite size measurement results of unmilled and mechanically activated ilmenite samples

Milling time (min)	Williamson-Hall		Warren-Averbach		Rietveld	
	$D_{v\ (nm)}$	ε (%)	$D_{s\ (nm)}$	RMSS (%)	Dv (nm)	ε (%)
0	346.63	0.13	239.60	0.10	183.00	0.08
20	72.98	0.61	43.15	0.39	70.28	0.35
45	42.02	1.08	19.60	0.85	37.20	0.65
90	14.60	1.44	5.45	0.78	17.10	0.97
150	8.01	1.43	4.45	0.78	11.18	1.04

3.4. Changes in lattice parameters

As indicated in Fig. 8, milling of ilmenite concentrate changes peak positions. The changes in peak position (2θ) leads to increase or decrees of d-spacing [27]. Figs. 10 and 11 show variations in unit cell volume and lattice parameters, respectively. These changes are coincide with variation of d-spacing. Unitcell software [28] was used to refine the lattice parameters of ilmenite by regression diagnostics method in Hexagonal system. After 45 min of milling, ilmenite lattice expands and then by extending the milling time unit cell volume shrinks. The sequence of unit cell expansion and shrinkage could be presumably due to the formation of lattice vacancy in the beginning of activation and then substitution of some atoms in lattice vacancies [29]. But another explanation for causes of lattice

volume variations is related to excess volume of grain boundary and interface tension. These two phenomena are present on the boundary of crystallites and could affect the lattice volume of the materials with nanometer scale microstructure[30, 31]. Based on the thermodynamic theories, interface tension creates compressive stress in the structure of the material which is inversely correlated with the crystallite size[31]. Compressive stress will increase by decreasing the crystallite size. Interfacial stress can be calculated in terms of grain boundary (GB) interfacial energy[32]. Milling process and the change of crystallite size lead to creation of excess GB energy in the crystallites interfaces. Excess GB energy can be calculated using Eq. (6) [33].

$$\gamma_{GB}^{Excess} = \frac{Gb^2 \rho d}{12(1-\pi)} \ln\left(\frac{d}{b}\right) \quad (6)$$

where G, b, ρ and d denote shear modulus, burger vectors, dislocation density and crystallite size, respectively. For ilmenite mineral G and b are 90 GPa and 0.5088 nm, respectively [34].

Disordered grain boundary in mechanically activated materials possesses some vacancies, which increases the grain boundary volume by a so-called excess free volume [35]. Excess free volume (ΔV) is calculated using Eq. (7) [36].

$$\Delta V = \frac{\left(d + \frac{\xi}{2}\right)^2 - d^2}{d^2} \quad (7)$$

where ξ is the grain boundary thickness ($\approx 1nm$) and d is the crystallite size. This free volume creates stress fields in the crystallites and the atoms can shift their position slightly toward the vacancies. If the excess volume effect is greater than the excess GB energy, then the lattice will expand, otherwise, the lattice will contract. In the present work, excess volume and excess GB energy were calculated as shown in **Fig. 12**. Final contraction of ilmenite unit cell and unit cell parameters indicate that the role of excess GB energy is dominant in comparison to the effect of excess free volume.

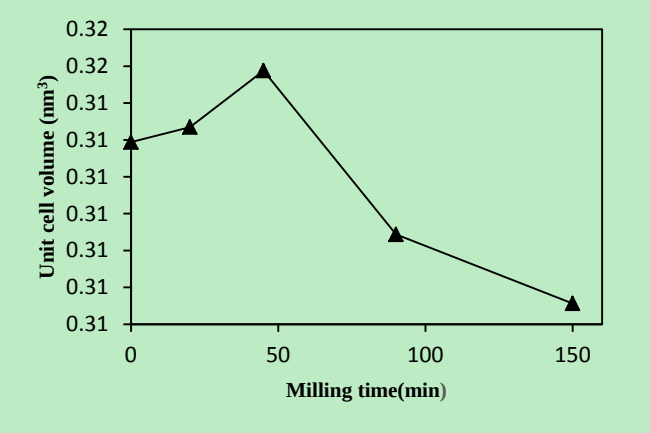

Fig. 10. Changes in the unit cell volume of milled ilmenite.

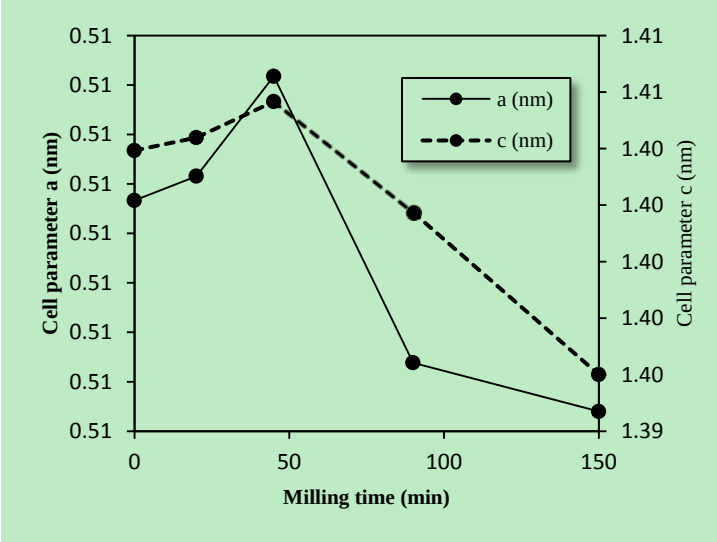

Fig. 11. Changes in the unit cell parameters of milled ilmenite.

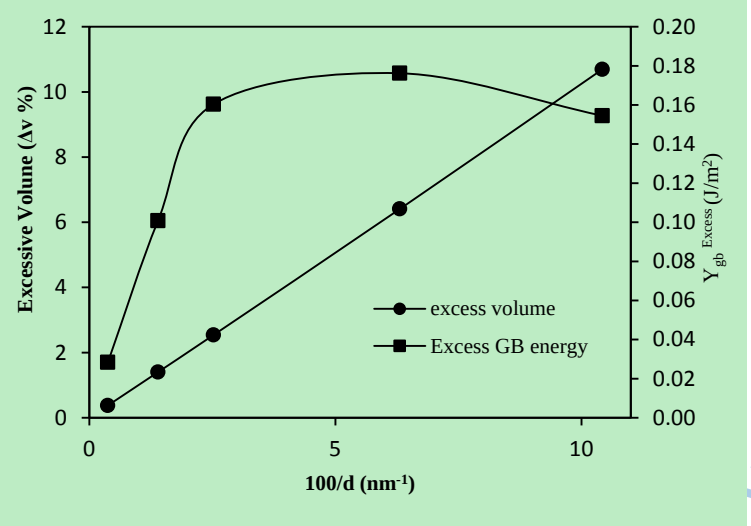

Fig. 12. Variations of excess free volume and excess GB energy versus crystallite size.

The X-ray amorphization of milled ilmenite were calculated using Eq. (8) as defined by Ohlberg and Strickler [37]:

$$A = 100 - X = 100 - \left(\frac{U_0}{I_0} \times \frac{I_x}{U_x} \times 100 \right) \qquad 8$$

In this formula, A is X-ray amorphization, U_x and U_0 denote the background of activated and non-activated samples while I_x and I_0 refer to integral intensities of diffraction lines of activated and non-activated samples, respectively. X is the degree of crystallinity. The term of X-ray amorphization degree refers to change of long-range order of material structure to the short-range order due to intensive milling which is not detectable by X-ray diffraction. Fig. 13 depicts X-ray amorphization degree of milled ilmenite and relative intensity of peaks as a function of milling time. The results indicate that the ilmenite structure was rapidly disordered through mechanical activation of ilmenite by the planetary ball mill whereas amorphization degree increased to 66% in the intensive milled for 20 min. By extending the milling to 150 min, the amorphization degree is maximized at 95%.

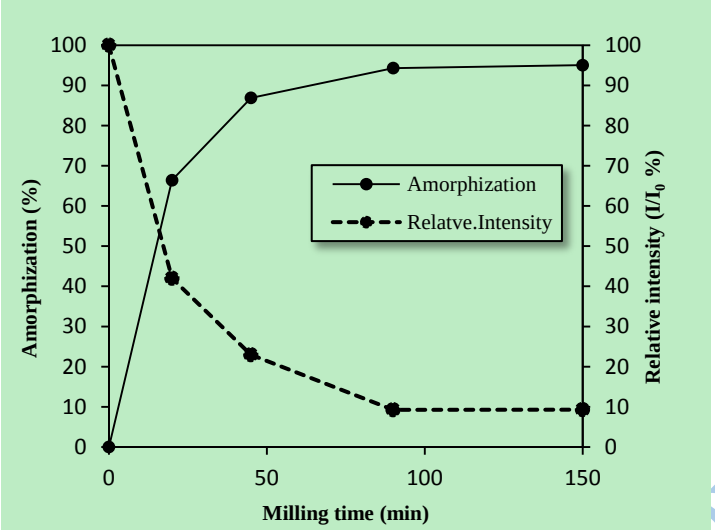

Fig. 13. Change in the X-ray amorphization degree and average relative intensity (I/I_0) of ground ilmenite

3.5. Stored energy

Mechanical activation makes structural changes in the bulk and surface of materials and leads to an increase in the enthalpy of materials. This excess enthalpy is the stored energy in the particle surface (ΔH_s), grain boundary (ΔH_{GB}), elastic strain (ΔH_ε), amorphous region (ΔH_A) and phase transferring (ΔH_{trans}). So the excess enthalpy could be presented as sum of the mentioned enthalpies as Eq. (9).

$$\Delta H_{excess} = \Delta H_s + \Delta H_{GB} + \Delta H_\varepsilon + \Delta H_A + \Delta H_{trans} \quad (9)$$

Detailed information for calculating each term of the Eq. (9) have been provided by Sasikumar et al. [38]. They calculated the stored energy for mechanically activated ilmenite and concluded that a major part of the energy is stored as strain energy, structural disorder and in defects with short relaxation times. However, our results based on long-lived defects as shown in **Table 3**, indicates that contribution of elastic strain energy in total stored energy is negligible and stored energy related to amorphization degree is more dominant.

Table 3

Stored energy and its distribution.

Milling time(min)	ΔHs (j/mol)	ΔH_{GB}(J/mol)	ΔHε(J/mol)	ΔH_A(KJ/mol)	ΔH_{Excess}(KJ/mol)
0	0	0	0.00	0	0
20	44.21	65.52	0.18	49.15	49.26
45	59.53	138.12	2.78	64.04	64.24
90	66.05	381.60	7.00	70.00	70.46
150	76.71	646.21	15.21	70.75	71.48

3.6. Reactivity

In order to briefly investigate the reactivity of mechanically activated ilmenite, non-activated and activated samples were leached by 50% (w/w) sulfuric acid at 80C° for 240 min. The extraction of Ti and the weight of leach residue are shown in Fig. 14. It can be seen that only 16.57% of Ti was leached from the non-activated sample while the extraction of Ti was increased to 92.95% from the mechanically activated sample for 150 min. As the leaching process was completed, severe weight loss in residue is observed. For achieving insight to changes in reaction kinetic as a result of mechanical activation, the leaching kinetic tests were performed as a function of leaching time up to 240 min. The obtained results are shown in Fig. 15. As presented, the extraction rate of Ti increases significantly in activated samples in compare to with non-activated sample. The rate of extraction at the initial stages of the leaching goes up rapidly in comparison with the rate of extraction at the prolonged stages. The extraction after 35 min of the leaching increased from 6.55% in the non-activated sample to 65.85% the mechanically activated sample for 150 min. The reactivity enhancement can be attributed to the structural changes of activated ilmenite.

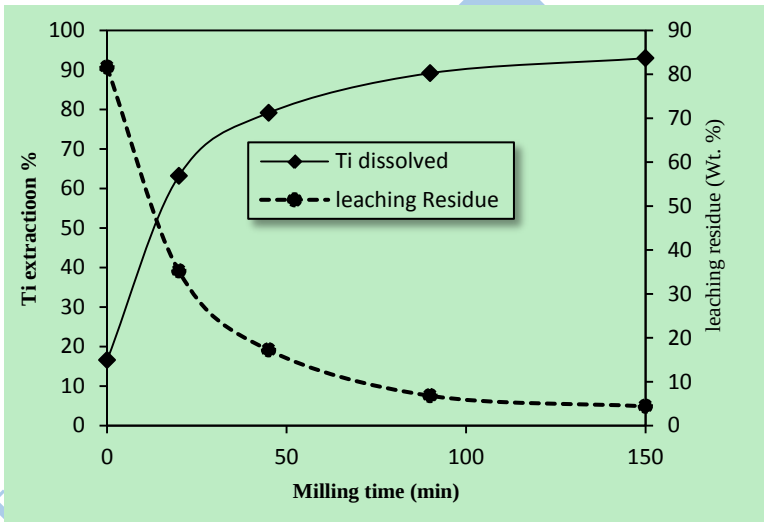

Fig. 14. Variation of Ti dissolved and leaching residue as function of milling time.

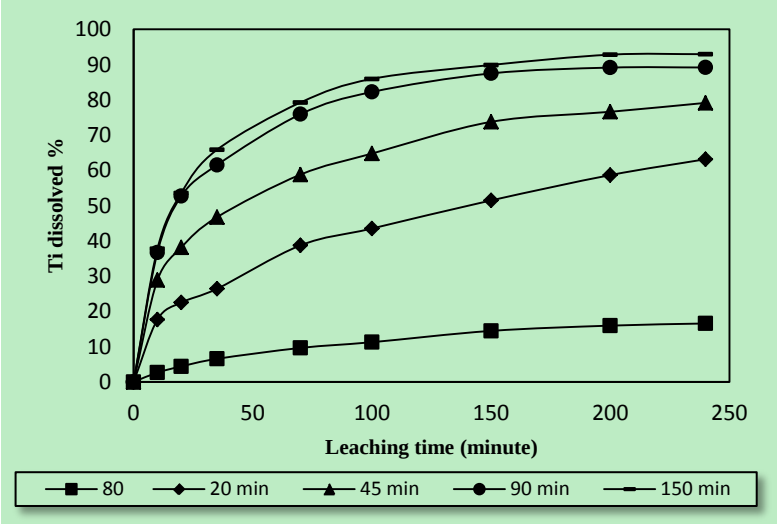

Fig. 15. Effect of milling time on dissolution of ilmenite.

Rate constant of dissolution reaction by sulfuric acid was estimated via kinetic experiments as shown in Fig. 16 vs. milling time. It is clear that the mechanical activation significantly accelerates the leaching process and leads to increasing the rate constant over 58 times in the mechanically activated sample for 150 min.

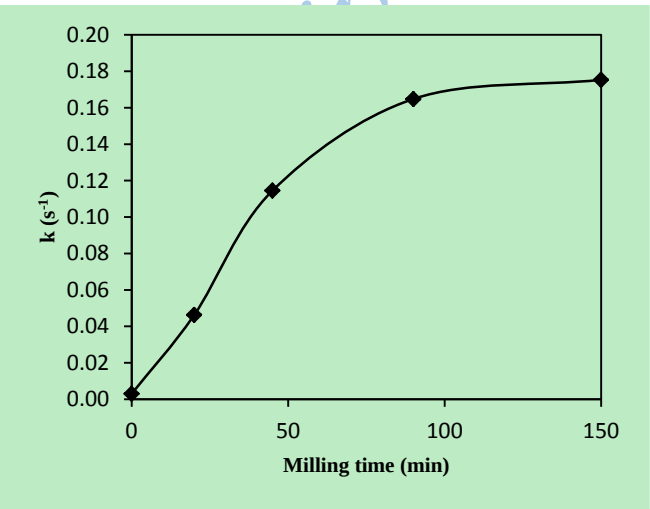

Fig. 16. Influence of the time of mechanical activation on the rate constant of ilmenite leaching.

Activation energy of ilmenite dissolution reaction for the non-activated and activated sample for 150 min was estimated using Arrhenius plots. The results are depicted in Fig. 17. Activation energy of 57.45 kJ/mol was calculated for un-milled ilmenite. Mechanical activation for 150 min decreases the activation energy to 41.09 kJ/mol. It can be concluded that reactivity and leaching kinetics of ilmenite as a main process in the production of

TiO_2 pigment can be improved by the mechanical activation of ilmenite due to a wide structural changes in ilmenite. However, the availability of structural characteristics at each step of leaching process is under investigation.

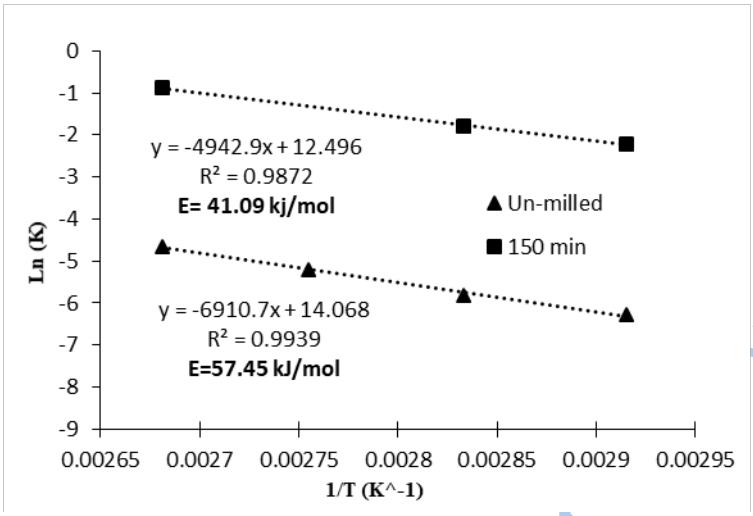

Fig. 17. Arrhenius plots of un-milled and 150 min milled ilmenite

4. Conclusions

Mechanical activation resulted a wide range structural changes in ilmenite structure and reactivity as follows:

1- BET surface area was increased up to 10.76 m^2/g in the milled ilmenite for 150 min. The fine particles were agglomerated with accessible pores after 45 min of intensive dry milling.

2- As s results, it was found that the surface-weighted crystallite size was 4.45 nm after 150 min in the planetary mill, corresponding to the volume-weighted crystallite size of 8 nm and 11.18 nm, obtained by Williamson-Hall and Rietveld methods, respectively. After 150 min mechanical activation, the root mean square strain, $< \varepsilon^2_{L=10nm} >^{1/2}$ was increased to 0.78%, corresponding to strain of 1.43% and 1.044% obtained by Williamson-Hall and Rietveld methods, respectively.

3- Detailed analysis indicated that the role of excess grain boundary energy is dominant in comparison to the effect of excess free volume of grain boundary so reduction of crystallite size leads to contraction of the ilmenite unit cell after 150 min.

4- After 150 min of intensive milling, the amorphization degree was reached to 95% and stored energy determination revealed that the contribution of x-ray amorphization into excess energy is dominant.

5- The rate constant of the dissolution reaction of ilmenite was increased over 58 times for the 150 min milled activated sample. Activation energy of ilmenite dissolution reaction was decreased from 57.45 kJ/mol in the non-activated ilmenite to 41.09 kJ/mol in the activated sample for 150 min.

6- The results suggest that mechanical activation would be successfully employed in the initial stage of TiO_2 pigment production, leaching, which is under investigation in our research center.

Acknowledgments

The support provided by the Mineral Processing Research Center of Sahand University of Technology is gratefully acknowledged. The authors also acknowledge the Iranian Mines & Mining Industries Development & Renovation, IMIDRO, for financial supporting of this research.

References:

[1] I. Lin, Implications of fine grinding in mineral processing mechanochemical approach, *J. Therm. Anal. Calorim.*,52(1998), No.2, p. 453.
[2] P. Baláž, *Extractive metallurgy of activated minerals*, Elsevier, 2000, p. 4-10.
[3] V. Boldyrev and K. Tkáčová, Mechanochemistry of solids: past, present, and prospects, *J. Mater. Synth. Process.*, 8(2000), No.3-4, p. 121.
[4] K. Tkáčová, *Mechanical activation of minerals*, Veda, 1989.
[5] C. Li, B. Liang and H. Wang, Preparation of synthetic rutile by hydrochloric acid leaching of mechanically activated Panzhihua ilmenite, *Hydrometallurgy*, 91(2008), No.1-4, p .121.
[6] C. Sasikumar, D. Rao, S. Srikanth, N. Mukhopadhyay and S. Mehrotra, Dissolution studies of mechanically activated Manavalakurichi ilmenite with HCl and H2SO4, *Hydrometallurgy*, 88(2007), No.1-4, p. 155.
[7] N. Welham and D. Llewellyn, Mechanical enhancement of the dissolution of ilmenite, *Miner. Eng.*, 11(1998), No.9, p. 835.
[8] Y. Chen, J. Williams, S. Campbell and G. Wang, Increased dissolution of ilmenite induced by high-energy ball milling, *Mater. Sci. Eng., A.*, 271(1999), No.1-2, p. 485.
[9] C. Li, B. Liang, L.-h. Guo and Z.-b. Wu, Effect of mechanical activation on the dissolution of Panzhihua ilmenite, *Miner. Eng.*, 19(2006), No.14, p. 1430.
[10] C. Sasikumar, D. Rao, S. Srikanth, B. Ravikumar, N. Mukhopadhyay and S. Mehrotra, Effect of mechanical activation on the kinetics of sulfuric acid leaching of beach sand ilmenite from Orissa, India, *Hydrometallurgy*, 75(2004), No.1-4, p. 189.
[11] L. Zhang, H. Hu, L. Wei, Q. Chen and J. Tan, Hydrochloric acid leaching behaviour of mechanically activated Panxi ilmenite (FeTiO3), *Sep. Purif. Technol.*, 73(2010), No.2.
[12] L. Zhang, H. Hu, L. Wei, Q. Chen and J. Tan, Effects of mechanical activation on the HCl leaching behavior of titanaugite, ilmenite, and their mixtures, *Metall. Mater. Trans. B.*, 41(2010), No.6, p. 1158.

[13] P. Pourghahramani and E. Forssberg, Comparative study of microstructural characteristics and stored energy of mechanically activated hematite in different grinding environments, *Int. J. Miner. Process.*, 79(2006), No.2, p. 137.
[14] P. Pourghahramani and M. A. Azami, Mechanical activation of natural acidic igneous rocks for use in cement, *Int. J. Miner. Process.*, 134(2015), p. 82.
[15] M. Senna, Determination of effective surface area for the chemical reaction of fine particulate materials, *Part. Part. Syst. Char.*, 6(1989), No.1-4.
[16] S. Krumm, WINFIT 1.2: version of November 1996 (The Erlangen geological and mineralogical software collection) of "WINFIT 1.0: a public domain program for interactive profile-analysis under WINDOWS", [in] *Proceedings of the XIII Conference on clay mineralogy and petrology, praha*, 1994, 253e261.
[17] J. I. Langford and A. Wilson, Scherrer after sixty years: a survey and some new results in the determination of crystallite size, *J. Appl. Crystallogr.*, 11(1978), No.2, p. 104.
[18] P. Pourghahramani and E. Forssberg, Microstructure characterization of mechanically activated hematite using XRD line broadening, *Int. J. Miner. Process.*, 79(2006), No.2, p. 108.
[19] B. E. Warren, *X-ray Diffraction*, Courier Corporation, 1969.
[20] B. Bourniquel, J. Sprauel, J. Feron and J. Lebrun, Warren-Averbach Analysis of X-ray Line Profile (even truncated) Assuming a Voigt-like Profile, [in] *Proceedings of the International Conference on Residual Stresses*, (1989), 184-189.
[21] H. Rietveld, A profile refinement method for nuclear and magnetic structures, *J. Appl. Crystallogr.*, 2(1969), No.2, p. 65.
[22] R. Young, Editor. The Rietveld Method, (1993).
[23] M. S. T. Degen, E. Bron, U. König, G. Nénert;, The HighScore suite, *Powder Diffraction* Volume 29(2014), No.Supplement S2.
[24] P. Pourghahramani and B. Akhgar, Characterization of structural changes of mechanically activated natural pyrite using XRD line profile analysis, *Int. J. Miner. Process.*, 134(2015), p. 23.
[25] J. Li and M. Hitch, Characterization of the microstructure of mechanically-activated olivine using X-ray diffraction pattern analysis, *Miner. Eng.*, 86(2016), p. 32.
[26] D. Balzar, Voigt-function model in diffraction line-broadening analysis, *Int. un. cryst. mono. cryst.*, 10(1999).
[27] C. Suryanarayana and M. G. Norton, X-ray diffraction: a practical approach. 1998.
[28] T. Holland and S. Redfern, Unit cell refinement from powder diffraction data: the use of regression diagnostics, *Mineral. Mag.*, 61(1997), No.1.
[29] E. F. Schubert, *Doping in III-V semiconductors*, E. Fred Schubert, 2015.
[30] R. Kumar, S. Bakshi, J. Joardar, S. Parida, V. Raja and R. Singh Raman, Structural Evolution during Milling, Annealing, and Rapid Consolidation of Nanocrystalline Fe–10Cr–3Al Powder, *Materials*, 10(2017), No.3, p. 6.
[31] W. Qin, T. Nagase, Y. Umakoshi and J. Szpunar, Lattice distortion and its effects on physical properties of nanostructured materials, *J. Phys.: Condens. Matter.*, 19(2007), No.23, p. 2.
[32] R. C. Cammarata and K. Sieradzki, Surface and interface stresses, *Annu. Rev. Mater. Sci.*, 24(1994), No.1, p. 215.
[33] A. Nazarov, A. Romanov and R. Valiev, Random disclination ensembles in ultrafine-grained materials produced by severe plastic deformation, *Scr. Mater.*, 34(1996), No.5, p. 729

[34] D. Tromans and J. Meech, Enhanced dissolution of minerals: stored energy, amorphism and mechanical activation, *Miner. Eng.*, 14(2001), No.11, p. 1363.
[35] M. Wagner, Structure and thermodynamic properties of nanocrystalline metals, *Phys. Rev. B*, 45(1992), No.2.
[36] P. Chattopadhyay, P. Nambissan, S. Pabi and I. Manna, Polymorphic bcc to fcc transformation of nanocrystalline niobium studied by positron annihilation, *Phys. Rev. B*, 63(2001), No.5.
[37] S. Ohlberg and D. Strickler, Determination of percent crystallinity of partly devitrified glass by X-ray diffraction, *J. Am. Ceram. Soc.*, 45(1962), No.4, p. 170.
[38] C. Sasikumar, S. Srikanth, N. Mukhopadhyay and S. Mehrotra, Energetics of mechanical activation–Application to ilmenite, *Miner. Eng.*, 22(2009), No.6, p. 572.